## Journal of Macromolecular Science, Part A

## Polyethylene Nanocomposites Obtained from *in-situ* Polymerization Using Supported Ziegler-Natta Catalyst System

Fu-An He[a]; Li-Ming Zhang[a]; Fan Yang[a]; Li-Shan Chen[a]; Qing Wu[a]

[a] Institute of Polymer Science, School of Chemistry and Chemical Engineering and Key Laboratory for Polymeric Composite and Functional Materials of Ministry of Education, Sun Yat-Sen (Zhongshan) University, Guangzhou, China

## PLEASE SCROLL DOWN FOR ARTICLE

# Polyethylene Nanocomposites Obtained from *in-situ* Polymerization Using Supported Ziegler-Natta Catalyst System

FU-AN HE, LI-MING ZHANG, FAN YANG, LI-SHAN CHEN, and QING WU

*Institute of Polymer Science, School of Chemistry and Chemical Engineering and Key Laboratory for Polymeric Composite and Functional Materials of Ministry of Education, Sun Yat-Sen (Zhongshan) University, Guangzhou, China*

The polyethylene nanocomposites were prepared by in-situ polymerization method using the Ziegler-Natta catalyst supported on the organoclay/$MgCl_2$ bisupport in the presence of $AlEt_3$ as the cocatalyst. The organoclay used is commercial Claytone APA. With XRD and TEM, the exfoliation of the layered silicate gallery of Claytone APA was confirmed. For the resulting polyethylene nanocomposites, the melting and crystallization behaviors were investigated by DSC, and their thermal property was examined in thermal oxidation condition.

**Keywords:** polyethylene; nanocomposites; clay; *in-situ* polymerization; melting; crystallization; thermal stability

## 1 Introduction

Polyolefins such as polyethylene (PE) and polypropylene (PP) are major plastics in the world-wide polymer industry. These commodity polymers have been produced with the Ziegler-Natta type or metallocene type organometallic coordination catalysts. In recent years, special interest has been devoted to develop their nanocomposites with layered silicates. It is well known that such materials have a pronounced increase in the properties such as tensile strength and heat resistance when compared to virgin polymer (1, 2). In order to obtain the polyolefin nanocomposite materials, several approaches including solution blending (3), melting intercalation (4–6) and *in-situ* polymerization (7–10) have been adopted.

In this work, we developed an *in-situ* exfoliation method for the preparation of the PE nanocomposites. Different from the intercalation-exfoliation strategy, the Ziegler-Natta catalyst components were first supported on the commercial organoclay (Claytone APA) to subsequently initiate the polymerization of ethylene on the organoclay surface. The structural characterization, melting and crystallization behavior, and the thermal oxidation property of the prepared PE nanocomposites are described here.

Address correspondence to: Li-Ming Zhang, Institute of Polymer Science, School of Chemistry and Chemical Engineering and Key Laboratory for Polymeric Composite and Functional Materials of Ministry of Education, Sun Yat-Sen (Zhongshan) University, Guangzhou 510275, China. E-mail: cedc61@zsu.edu.cn; ceszhlm@mail.sysu.edu.cn

## 2 Experimental

### 2.1 Materials

The commercial organoclay was obtained from Southern Clay Products Inc. (Gonzales, Texas) under the trade name of Claytone APA. It was received as a fine particle powder. According to Salahuddin and Shehata, (11) the modified silicate was produce by a cation exchange reaction between the silicate and dimethyl benzyl hydrogenated tallow ammonium chloride, and the percentage of organic content (dimethyl benzyl hydrogenated tallow ammonium chloride) was 24%. Compared with common Cloisites organoclay, Claytone APA is characteristic of high efficiency and can be used in high nonpolarity systems. Before preparing the supported catalysts, the organoclay was dried in vacuum for 24 h. Triethyl aluminum ($AlEt_3$) was taken as 400 g/l solutions in heptane. Ethanol, tetrahydrofuran (THF) and heptane were distilled and dried over molecular sieves before use. $TiCl_4$ and $MgCl_2$ were used as received without further purification.

### 2.2 Preparation of Supported Catalysts

In a typical experiment, 1.0 g of anhydrous $MgCl_2$ was introduced into a glass reactor equipped with a magnetic stirrer, then 20 ml tetrahydrofuran (THF) and 1.5 ml absolute ethanol were added. The mixture was heated to 45°C and stirred overnight until the $MgCl_2$ was completely dissolved. 3.0 g of the organoclay was then introduced and was uniformly dispersed in the solution under magnetic stirring. After being stirred at 45°C for 2 h, the agglomerated particles

were separated by decanting, washed with heptane and dried under vacuum at 60°C for 2 h. The calculated amount of TiCl$_4$ was then added to the above bissupport suspended in 15 ml of heptane. The suspension was stirred at 45°C for 2 h. After decantation, the solid was washed with heptane several times, and then dried under vacuum. The supported complex was obtained as solid, yellow particles.

### 2.3  Ethylene Polymerization

50 ml of toluene, and a solution of AlEt$_3$ were introduced into a 100 ml glass reactor equipped with a magnetic stirrer in succession. After that, the supported catalyst was added and the [Al]/[Ni] molar ratio was kept to be 100. The polymerization was carried out under a constant ethylene pressure of 106.7 kPa at 50°C for a given reaction time, and then terminated with acidified ethanol. The precipitated products were washed up with ethanol and dried under vacuum at 60°C for 6 h. Polyethylene nanocomposites with various organoclay loadings, namely PEC1 (2.29 wt% organoclay), PEC2 (5.50 wt% organoclay), PEC3 (8.73 wt% organoclay), were obtained by controlling the polymerization time. The organoclay loading (wt%) in the nanocomposites was determined by TGA in nitrogen. For a comparative study, the pure polyethylene was obtained by using the Ziegler-Natta catalyst, only supported on MgCl$_2$ under the same polymerization conditions.

### 2.4  Characterization

A Rigaku (Japan) D/max-RB wide-angle X-ray diffractometer (WAXD) was used to characterize the layer structure of the clay in the nanocomposites. The operation parameters were Cu-K$\alpha$ radiation at a generator voltage of 40 kV and a current of 100 mA. The scanning rate was 2/min at an interval of 0.02°. The nanoscale dispersion of the clay platelet was investigated by a JEM-100CX II transmission electron microscopy with an acceleration voltage of 100 kV. The ultrathin slides were obtained by sectioning the compression-molded sample along a direction perpendicular to the compression under cryogenic condition. The thermal stability was investigated by thermogravimetric analysis using NetzschTG-209 in air at a purge rate of 50 ml/min. The heating rates were set as 10, 20, and 30°C/min and the scanning temperature was in the range from 50°C to 700°C. The melting and crystallization behaviors of the PE and its nanocomposites were studied using a Perkin-Elmer DSC-7 under a nitrogen atmosphere. In order to eliminate the influence of thermal history and the effect of thermal treatment on the crystalline structure of polyethylene, all samples were first heated to 160°C for 5 min, then cooled to 50°C and reheated to 160°C, all at a rate of 20°C/min.

## 3  Results and Discussion

### 3.1  Microstructure Characteristics

The FTIR spectra of PE and its nanocomposites are illustrated in Figure 1. The spectrum of the PE nanocomposites clearly exhibits the characteristic absorptions attributed to both the polyethylene and the clay. The IR absorption bands at 2912 cm$^{-1}$ and 2850 cm$^{-1}$ represent CH$_2$ stretching vibrations, and the bands at 1462 cm$^{-1}$ and 717 cm$^{-1}$ correspond to the bending and rocking vibration of CH$_2$, respectively. The absorption bands at 3640 cm$^{-1}$, 1047 cm$^{-1}$, 521 cm$^{-1}$ and 460 cm$^{-1}$ are O-H stretching, Si-O stretching, Al-O stretching and Si-O bending vibrations for the organoclay, respectively. These FTIR assignments verify that the organoclay has been doped into the polyethylene matrix during the polymerization process.

Figure 2 displays the XRD patterns of the organoclay and the PE nanocomposites. The characteristic X-ray peak (001) of claytone APA was around 4.72°, which corresponds to a basal spacing of 1.87 nm and is identical to that reported by Salahuddin and Shehata (11). In contrast, the XRD patterns of the PE nanocomposites did not include any 001 diffraction peak, which means either that an exfoliated nanocomposite has been produced or that the long-range-ordered structure of clay had been destroyed during the preparation process.

The morphology of the PE nanocomposites was studied by transmission electron microscopy (TEM). Figure 3 shows the TEM micrographs of PEC2, which contains 5.50 wt% of the organoclay. The white areas represent the PE matrix and the black ones the organoclay. From the higher magnification TEM image, the individual silicate layer was observed, as indicated by the dark arrow. From lower magnification TEM image, it was found that the organoclay platelets could be well dispersed in the PE matrix and no obvious aggregation occurred. These facts demonstrate that the obtained PE nanocomposite has an exfoliated structure.
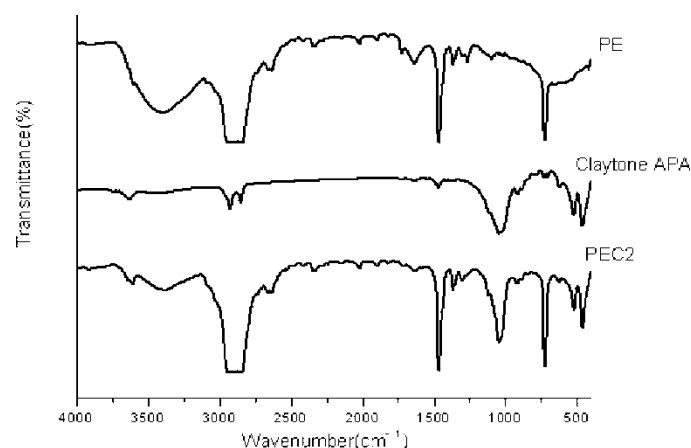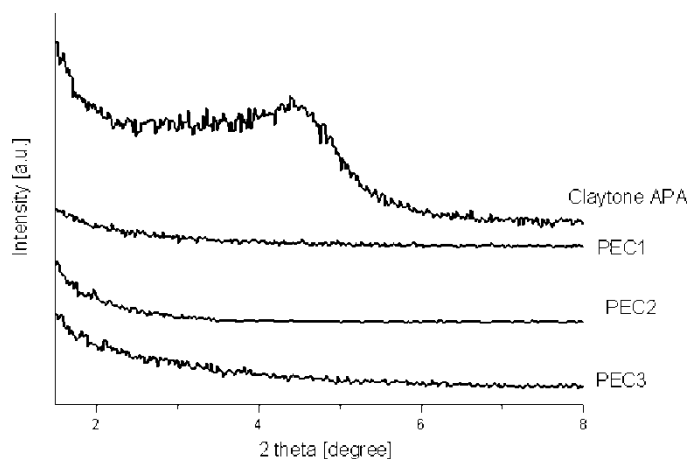


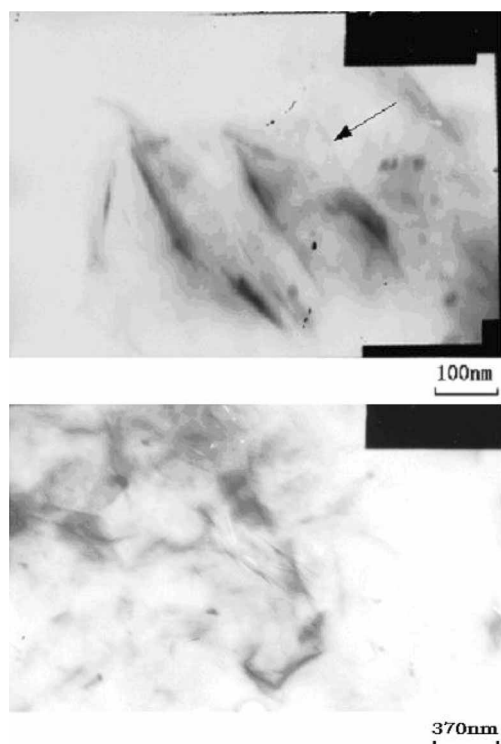**Fig. 1.**   The IR spectra of PE, claytone APA and PEC2.

**Fig. 2.** XRD patterns of claytone APA and the polyethylene nanocomposites.

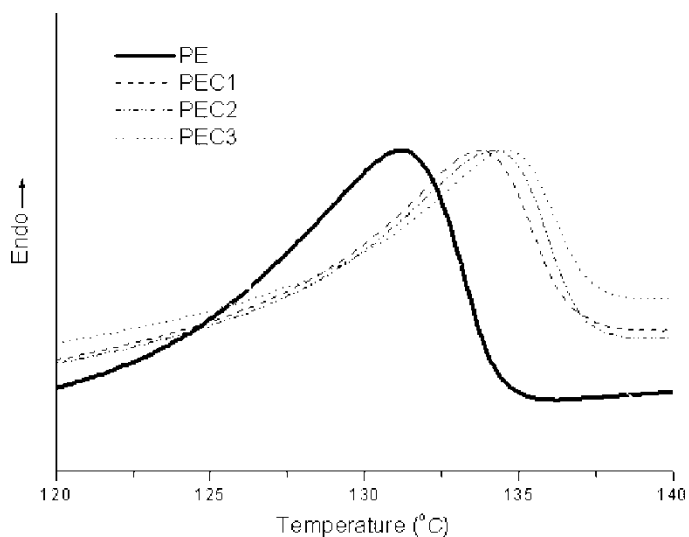### 3.2 Melting and Crystallization Behavior

The non-isothermal crystallization exothermic and endothermic curves of PE and its nanocomposites are illustrated in Figures 4 and 5, respectively. The values of the peak melting temperature ($T_m$), the heat evolved during crystallization ($\Delta H_m$), the degree of crystallinity ($X_c$) and the peak crystallization temperature ($T_c$) at a cooling rate of 20°C/min for PE and its nanocomposites are listed in Table 1. The degree of crystallinity ($X_c$) can be calculated



**Fig. 3.** TEM micrographs of PEC2.



**Fig. 4.** Heating scans for neat PE and its nanocomposites.

from the heat evolved during crystallization ($\Delta H_m$) with the following relation:

$$X_c\,(\%) = \frac{\Delta H_m}{(1 - \Phi)\Delta H_m^0} \times 100 \qquad (1)$$

where $\Delta H_m^0$ is the heat of fusion for 100% crystalline polyethylene and $\Phi$ is the weight fraction of the filler in the nanocomposites. The heat of fusion for 100% crystalline of polyethylene is taken as 286 J/g. The results show that both $T_m$ and $X_c$ decreased significantly upon the exfoliation of the clay layers. This decrease may be attributed to a higher interfacial area and adhesion between the PE and the nano-scale clay layers, which would act to reduce the mobility of
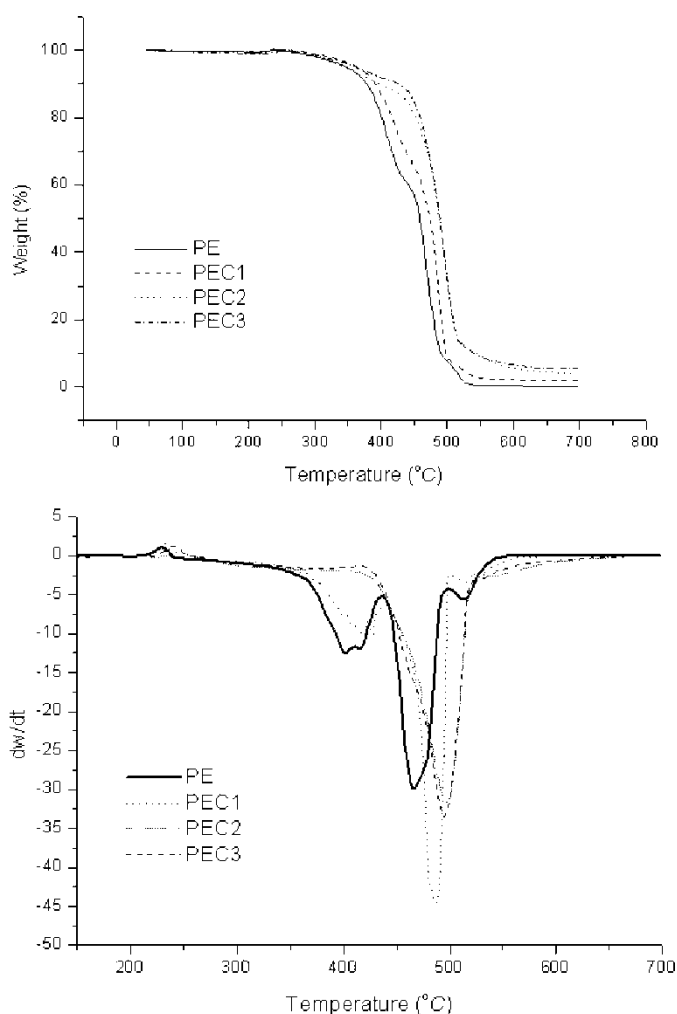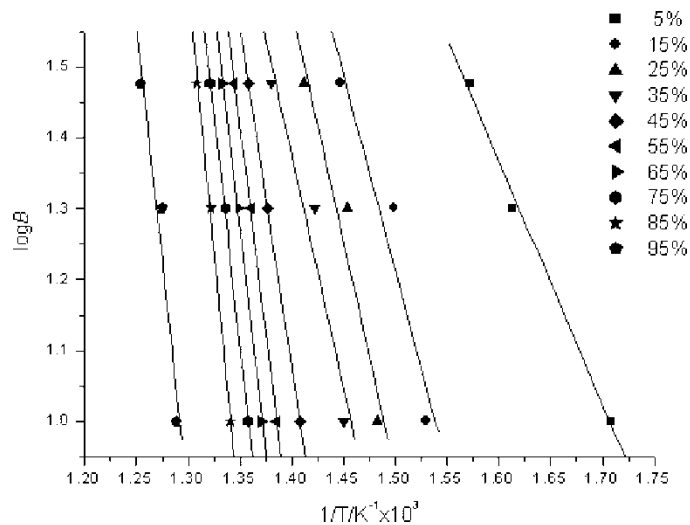


**Fig. 5.** Cooling scans for neat PE and its nanocomposites.

**Table 1.** Values of $T_m$, $\Delta H_m$, $X_c$ and $T_c$ for PE and its nanocomposites

| Sample | $T_m$ (°C) | $\Delta H_m$ (J/g) | $X_c$ (%) | $T_c$ (°C) |
|--------|-----------|--------------------|-----------|-----------|
| PE | 131 | 186.63 | 65.3% | 113 |
| PEC1 | 133 | 161.66 | 56.5% | 115 |
| PEC2 | 134 | 113.69 | 39.8% | 116 |
| PEC3 | 135 | 116.18 | 40.2% | 117 |

crystallizable chain segments. On the other hand, $T_c$ of all nanocomposites is higher than that of neat PE. This phenomenon could be explained by the heterogeneous nucleation effect of the organoclay nanoparticles on the PE macromolecule segments, which leads to the crystallization of PE macromolecule segments at a higher crystallization temperature.



**Fig. 7.** Plot of $\log\beta$ vs. $1/T$ for PE.

### 3.3 *Thermal Oxidation Stability*

Figure 6 shows the TG and DTG curves from the thermal degradation of PE and its nanocomposites under an air atmosphere at a scan rate of 20°C/min. With the increase of the organoclay loading, the number of degradation stages decreased. When 30% wt loss was selected as a point of comparison, the thermal-oxidative decomposition temperatures for PE, PEC1, PEC2 and PEC3 were found to be 417, 438, 469 and 471°C, respectively. This fact showed that the thermal oxidation property of the PE nanocomposites was better than that of neat PE, and could be improved with the increase of the organoclay loading. In order to obtain a better insight into the thermal-oxidative stability of the PE nanocomposites, the kinetics of the thermo-oxidation degradation process were analyzed. For this purpose, the following



**Fig. 6.** TG and DTG curves for PE and its nanocomposites under an air atmosphere.
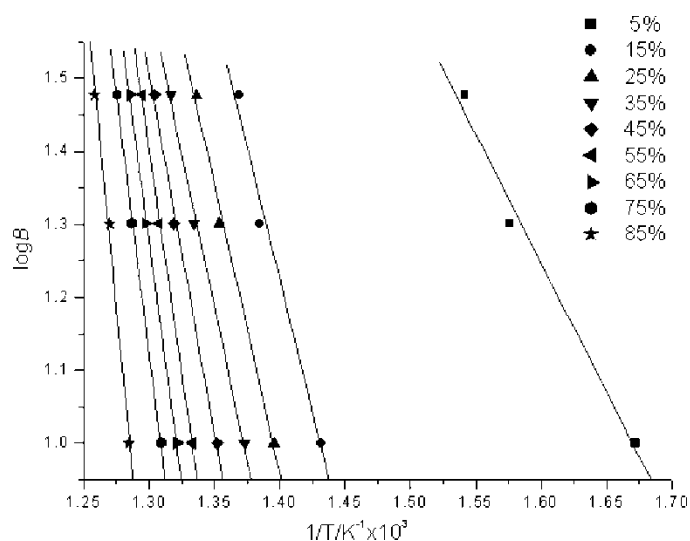


**Fig. 8.** Plot of $\log\beta$ vs. $1/T$ for PEC3.

**Table 2.** The Ea values for PE and its nanocomposites and the corresponding determination

| Weight loss (%) | PE | | PEC1 | | PEC2 | | PEC3 | |
|---|---|---|---|---|---|---|---|---|
| | $Ea$ (kJ · mol$^{-1}$) | $R$ | $Ea$ (kJ · mol$^{-1}$) | $R$ | $Ea$ (kJ · mol$^{-1}$) | $R$ | $Ea$ (kJ · mol$^{-1}$) | $R$ |
| 5 | 62.6 | 0.997 | 63.4 | 0.992 | 43.2 | 0.982 | 64.4 | 0.993 |
| 15 | 100.5 | 0.955 | 86.7 | 0.984 | 99.1 | 0.989 | 133.0 | 0.990 |
| 25 | 119.4 | 0.967 | 96.6 | 0.985 | 156.7 | 0.981 | 144.2 | 0.997 |
| 35 | 119.8 | 0.966 | 152.3 | 0.998 | 223.1 | 0.998 | 153.1 | 0.998 |
| 45 | 175.3 | 0.999 | 222.6 | 0.996 | 294.4 | 0.995 | 179.8 | 0.998 |
| 55 | 212.0 | 0.999 | 267.1 | 0.985 | 299.6 | 0.998 | 224.7 | 0.999 |
| 65 | 228.3 | 0.997 | 286.1 | 0.977 | 332.7 | 0.995 | 241.4 | 0.999 |
| 75 | 237.8 | 0.999 | 265.2 | 0.989 | 264.8 | 0.999 | 257.2 | 0.998 |
| 85 | 271.5 | 0.998 | 247.1 | 0.995 | 295.8 | 0.999 | 333.4 | 0.996 |
| Average | 169.5 | | 187.2 | | 223.3 | | 194.3 | |

Flynn−Wall−Ozawa equation (12) was used:

$$\log \beta = \log\left[\frac{AE}{g(\alpha)R}\right] - 2.315 - 0.457\frac{E}{RT} \qquad (2)$$

where $g(\alpha)$ is the conversion functional relationship, $A$ is the preexponential factor (min$^{-1}$), $E$a is the activation energy (kJ/mol), $R$ is the gas constant, $\beta$ is the heating rate (°C/min), and $T$ is the absolute temperature (K). $Ea$ could be calculated from the slope of the straight line obtained by drawing the dependence $\log\beta$ vs. $1/T$ at different conversion degrees. Figures 7 and 8 give the respective plots of $\log\beta$ vs. $1/T$ for PE and PEC3 at some fixed weight loss. The $Ea$ values calculated from the slopes of the straight lines for PE and its nanocomposites are listed in Table 2. The average $Ea$ values for PE, PEC1, PEC2 and PEC3 were determined to be 169.5, 187.2, 223.3 and 194.3 kJ/mol, respectively. These results show that the presence of the exfoliated clay nanolayers increases the $Ea$ of the thermo-oxidative degradation process of the PE matrix.

## 4  Conclusions

PE nanocomposites could be obtained by in-situ polymerization method using the Ziegler-Natta catalyst supported on the organoclay/MgCl$_2$ bisupport in the presence of AlEt$_3$ as the cocatalyst. Their exfoliation structure was confirmed by XRD and TEM. The addition of nanoscale clay particles influences significantly the melting and crystallization behavior of the PE matrix. In addition, the nanoscale dispersion of clay platelets in the PE matrix improved the thermal oxidation stability.

## 6  References

1. Beall, G.W. Ed. *Polymer-Clay Nanocomposites*; Wiley: New York, 2000.
2. Krishnamoorti, R. and Vaia, R.A. Ed. Polymer Nanocomposites, American Chemical Society: Washington, DC, 2001.
3. Jeon, H.G., Jung, H.T., Lee, S.W. and Hudson, S.D. (1998) *Polym. Bulletin*, **41**, 107.
4. Zhao, C., Qin, H., Gong, F., Feng, M., Zhang, S. and Yang, M. (2005) *Polym. Degrad. Stab.*, **87**, 183.
5. Gopakumar, T.G., Lee, J.A., Kontopoulou, M. and Parent, J.S. (2002) *Polymer*, **43**, 5483.
6. Zanetti, M., Bracco, P. and Costa, L. (2004) *Polym. Degrad. Stab.*, **85**, 657.
7. Heinemann, J., Reichert, P., Thomann, R. and Mulhaupt, R. (1999) *Macromol. Rapid. Commun.*, **20**, 423.
8. Alexandre, M., Dubois, P., Sun, T., Garces, J.M. and Jerome, R. (2002) *Polymer*, **43**, 2123.
9. Yang, F., Zhang, X., Zhao, H., Chen, B., Huang, B. and Feng, Z. (2003) *J. Appl. Polym. Sci.*, **89**, 3680.
10. Jin, Y.H., Park, H.J., Im, S.S., Kwak, S.Y. and Kwak, S. (2002) *Macromol. Rapid. Commun.*, **23**, 135.
11. Salahuddin, N. and Shehata, M. (2001) *Polymer*, **42**, 8379.
12. Ozawa, T. (1965) *Bull. Chem. Soc. Jpn.*, **38**, 1881.